© 2018 IJSRSET | Volume 4 | Issue 1 | Print ISSN: 2395-1990 | Online ISSN : 2394-4099
Themed Section : Engineering and Technology

ANFIS Controller Based Five-Leg AC-DC-AC Converter-Fed Induction Motor Drive

Areti Gopi
M. Tech Scholar Department of Electrical & Electronic Engineering: Nova College of Engineering & Technology, Jupudi, Andhra Pradesh, India

ABSTRACT

AC-DC-AC converter-fed induction motor drive is for the most part acknowledged by back-to-back three-phase converters. Be that as it may, fault in a single semiconductor switch will make it inoperative. To empower proceeded with controllable operation if there should arise an occurrence of the issues happening in the converter, the five-leg converter with a shared leg between the grid and load sides is a conceivable arrangement. Be that as it may, this topology represents ainherent two-objective control issue since its grid and load sides ought to be controlled all the while. In this paper, new control scheme in view of the FCS-MPC combined with intrinsic characteristics for the five-leg converter is existed for autonomous control of the rectifier and inverter subsystem with the shared leg over current imperative. Another novel ANFIS control is proposed in this paper and with a specific end goal to give a total assessment of the proposed ANFIS control scheme, the traditional MPC control plot is directed for comparison. Simulation results about are given to approve the adequacy of the proposed scheme.

Keywords : Induction Motor, ANFIS,FCS-MPC.

I. INTRODUCTION

THE induction motor (IM) has turned out to be one of the primary actuators for modern applications on account of its cost, reliability, roughness, straightforwardness, productivity, and simplicity of fabricate. The back-back three-phase converters help to accomplish superior from an IM [1], particularly in the high-control regenerative drives. In any case, this converter is delicate to control switch fault. In AC-DC-AC converters, these disappointments can happen at the frontend rectifier or at the output inverter. To enhance the reliability quality of the IM drives, fault tolerant plans for AC-DC-AC converter must be actualized. One of the option plans is to include equipment repetition into the systems. Be that as it may, it is a costive, weight and space devouring arrangement [2]. In this way, another healing arrangements actualized by real timefault identification and converter reconfiguration has a steady improvement amid the previous decade, known as nonredundant fault tolerant structures.

On account of the nonredundant fault working structures, the converter can be produced either with a DC-bus midpoint association[3] or with a common leg imparted to another motor drive [4] or rectifier [5] to supply the motor drive. The DC-bus mid-point association strategy will definitely cause the capacitor voltage variance and additional endeavors must be paid to adjust for this change, while the shared leg case, this issue is kept away from. With shared-leg topology, the disappointment of one leg in the input rectifier or one leg in the inverter can be viably overseen. As an outcome, a few papers in view of pulse width modulation (PWM) procedures were distributed [5]. A PWM procedure for applications in which the loadfrequency was equivalent to the

gridfrequency (e.g., UPS applications) was proposed to accomplish conceivable control of this topology. Be that as it may, this technique lost the value of variable frequency in inverter since the gridfrequency was constantly steady. Two leg-to-leg rather than three leg-toneutral regulated voltages were proposed in [5] to control the rectifier/inverter autonomously. Be that as it may, since some legto-leg regulation examples had no comparable leg-to-impartial exchanging designs in the five leg converter, the estimated calculation received in choosing exchanging examples would prompt a ton of current ripples. The high common modevoltage which prompted current symphonious misfortunes was appeared. All the more imperatively, the possibly overcurrent in the common leg was not considered in these papers. As a conceivable arrangement, a model prescient control plot for the synchronous control of the rectifier and inverter is considered in this paper. Limited control-set model prescient control (FCS-MPC) was as of late proposed as a successful plan in superior control of the power converters, for example, factor speed engine drives [6], grid converter,back-back converter and other power electronic converter setup. No paper to the best of creators' input has any past endeavor to use FCS-MPC in conjunction with a five-leg AC-DC-AC converter-sustained acceptance engine.

In this paper, the model of the five-leg AC-DC-AC converter is broke down, and a control scheme in view of FCS-MPC is proposed for elite control of a five-leg converter-nourishedinductionmotor. Indeed, with an extremely adaptable structure of cost work in FCS-MPC, it is conceivable to include the limitation (e.g., shared-leg overcurrent) and other control targets. A FCS-MPC with bring down figuring load created from the innate normal for the five-leg converter is proposed for pragmatic usage.
The voltage restriction of the fiveleg AC-DC-AC converter is examined and the speeds extend for free control of the rectifier and motor is given.

II. MODELING OF THE FIVE-LEG AC-DC-AC DRIVE

Without loss of simplification, it is accepted that all through the paper, when the switch faults happen in the phase l3 of the inverter, the comparing motorphase that lost the supply is associated with the leg g3 of the rectifier for faulttolerant operation, as appeared in Figure 1.

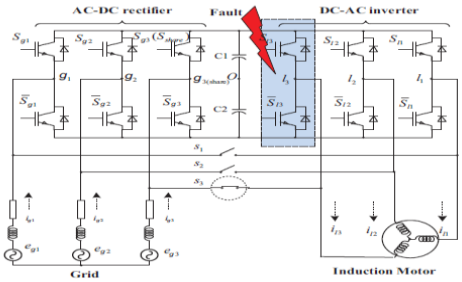

Figure 1. AC-DC-AC converter-fed motor drive with reconfiguration

In five-leg AC-DC-AC drive framework considered in this paper (Figure 1), one side of the converter is associated with a three-phase adjusted sinusoidal source, and the opposite side of the converter is associated with a three-phase acceptance machine. The leg g3 is shared by the two sides.

Keeping in mind the end goal to determine the proposed control plot, the five-leg back-back converter is considered as a three-phase dynamic front-end rectifier and a three-phase inverter. The dynamic frontend rectifier essentially works as a boost chopper (frequently called a boost rectifier) with AC voltage at the input, however dc voltage at the output, keeping up sinusoidal line current. The threephase inverter gets dc voltage and proselytes it to ac voltage for the engine drive. The point by point model of each part will be explained in the accompanying content.

A. Five-Leg Converter Model

In this paper, the converter is considered for execution by perfect switches (i.e., with no dead time and no voltage drop). Subsequently, exchanging

conditions of any converter legs can be composed as takes after:

$$S_x = \begin{cases} 1, \text{if the xth leg upper switch is on} \\ 0, \text{if the xth leg lower switch is on} \end{cases}$$

$x = g1, g2, g3(\text{share}), l_1, \text{and } l_2$ (1)

B. Three-Phase Active Front-End Rectifier Model

The continuous-time model of a three-phase active front-endrectifier can be expressed by the following equation:

$$\frac{d\vec{i}_g(t)}{dt} = -\frac{R_g}{L_g}\vec{i}_g(t) + \frac{1}{L_g}\vec{e}_g(t) - \frac{1}{L_g}\vec{v}_g(t) \quad (2)$$

Where$\vec{i}_g = i_{g\alpha} + j.i_{g\beta}$ is the input current vector, is the grid voltage vector, $\vec{v}_g = v_\alpha + j.v_\beta$ is thevoltage vector generated by the active front-end rectifier, $R_g$is the equivalent series resistance, $L_g$is the filter inductance.The predicted grid current is calculated by the followingdiscrete-time equation

$$\vec{i}_g(k+1) = \left(1 - \frac{R_g T_s}{L_g}\right)\vec{i}_g(k) + \frac{T_s}{L_g}\vec{e}_g(k) - \frac{T_s}{L_g}\vec{v}_g(k) \quad (3)$$

Which is obtained from the discretizing (2) for a sampling timeTs . Since the control variables of the rectifier is the activeand reactive power.

Considering the input voltage and current vectors in orthogonalcoordinates, the predicted instantaneous input active andreactive power are given with

$$P(k+1) = \mathrm{Re}\{\vec{e}_g(k+1)\bar{\vec{i}}_g(k+1)\} \quad (4)$$

$$Q(k+1) = \mathrm{Im}\{\vec{e}_g(k+1)\bar{\vec{i}}_g(k+1)\} \quad (5)$$

For a high sampling frequency in this paper, with regard tothe grid fundamental frequency, it can be assumed that$e_g(k+1) \approx e_g(k)$.

C. Induction Motor Model

The dynamic model of an induction motor viewing fromthe stator reference frame can be given as follows:

$$0 = R_r\vec{i}_r + \frac{d\psi_r}{dt} - j\omega\vec{\psi}_r \quad (6)$$

$$\vec{v}_s = \frac{d\psi_s}{dt} + R_s\vec{i}_l \quad (7)$$

$$\vec{\psi}_r = L_m\vec{i}_l + L_r\vec{i}_r \quad (8)$$

$$\vec{\psi}_s = L_s\vec{i}_l + L_m\vec{i}_r \quad (9)$$

$$T_e = \frac{3}{2}p\vec{\psi}_s \times \vec{i}_l \quad (10)$$

Where L_m and L_s (L_r) refer to shared and stator (rotor)inductance, while $\vec{i}_l(\vec{i}_r)$ represent the stator (rotor) current,R_s (R_r) and $\vec{\psi}_s(\vec{\psi}_r)$denote stator (rotor) resistance and stator(rotor) flux, T_e and p denote torque and number of the polepairs, $\vec{v}_s$ and ω represent the stator voltage and rotor electricalspeed. Since the measured variables are stator currents androtor speed, all the other quantities are either estimated orpredicted. As the stator flux is not measurable, stator flux isestimated from rotor flux by substituting $\vec{i}_r$ in (9) to (8)

$$\vec{\psi}_s = \frac{L_m}{L_r}\vec{\psi}_r + \sigma L_s\vec{i}_l \quad (11)$$

Wherethe σdenote the leakage factor. The $\vec{\psi}_r$can be obtainedby substituting $\vec{i}_r$in (6) to (8)

$$\vec{\psi}_r + \tau_r\frac{d\vec{\psi}_r}{dt} = L_m\vec{i}_l + j\omega\tau_r\vec{\psi}_r \quad (12)$$

Where $\tau_r = L_r/R_r$ is the rotor time constant. Since the controlvariable of the induction motor drive is stator flux and torque,these values should be predicted at sampling time instant k+1.The stator flux can be predicted by discretizing (7)

$$\vec{\psi}_s(k+1) = \vec{\psi}_s(k) + T_s\vec{v}_s(k) - R_sT_s\vec{i}_l(k) \quad (13)$$

The torque can be predicted by

$$T_e(k+1) = \frac{3}{2}p.\mathrm{Im}\{\vec{\psi}_s(k+1)^*.\vec{i}_l(k+1)\} \quad (14)$$

Where the predicted stator current can be obtained fromequation (6)-(9)

$$\vec{i}_l(k+1) = \left(1 + \frac{T_s}{\tau_\sigma}\right).\vec{i}_l(k) + \frac{T_s}{T_s+\tau_\sigma}.\left\{\frac{1}{R_\sigma}\left(\left(\frac{k_r}{\tau_r} - j\omega(k)k_r\right)\vec{\psi}_r(k) + \vec{v}_s(k)\right)\right\} \quad (15)$$

Where $k_r = L_m/L_r$ is the rotor coupling factor, $R_\sigma = R_S + k_r^2R_r$refers to the equivalent resistance, $T_\sigma = \sigma L_s/R_\sigma$denotes the equivalent time constant.

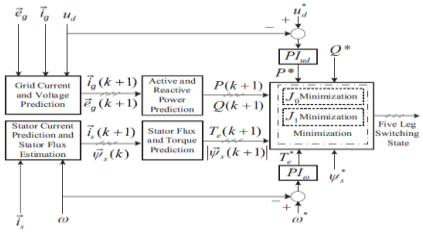

Figure 2. Control block diagram of the FCS-MPC

III. FCS-MPC CONTROL SCHEME

In FCS-MPC, the control goals are characterized as the cost work, making the FCS-MPC plot with a superb capacity to manage the multi-input multi-output (MIMO) framework. It can treat the five-leg AC-DC-AC converter as onesystem. The inward circles of rectifier and inverter subsystems are controlled by one cost work. The order dc link voltage u_d^* is contrasted and the genuine u_d and the mistake motion through a PI controller is used to create the dynamic power charge while the summon speed ω^* is contrasted and the real ω also, the mistake motion through a PI controller is used to create the torque summon. The entire control square of the proposed scheme is given in Figure 2. In standard FCS-MPC, all attainable inputvoltage vectors comparing to the conceivable exchanging states are assessed, and the one with the most reduced cost work esteem will be connected in the following testing time frame. Be that as it may, a five-leg converter has 32 exchanging states. An entire assessment of the standard FCS-MPC requires 32 sets variable forecast and cost work advancement. With the substantial calculation trouble, the testing frequency is constrained, which prompt huge output current willripple.

To take care of this problem, a FCS-MPC with bring down computational weight must be actualized. At long last, by assessing the cost capacities at two differentcommon leg expresses, the ideal exchanging condition of the five-leg converter framework can be resolved.

A. Cost Function Design

As per the switching condition of the shared leg, the cost elements of the rectifier and the inverter should be figured twice. Every assessment requires 8 sets variable forecast and cost work streamlining (four sets for rectifier and four sets for inverter). Along these lines, with regards to the dynamic front-end rectifier subsystem, the cost work, intended to control the dynamic and receptive power, can be given by

$$J_{grid} = \frac{|P^* - P(k+1)_i|}{P_N} + \frac{|Q^* - Q(k+1)_i|}{P_N}, \quad i\epsilon\{1,2,3,4;5,6,7,8\} \qquad (16)$$

Where P^*andQ^* are, separately, the future references of dynamic power and receptive power at skyline k+1, PN is the greatest output energy of the rectifier. With regards to the enlistment engine drive subsystem, the cost work, intended to control the stator motion and torque, can be given by

$$J_{load} = \frac{|T_e^* - T_e(k+1)_i|}{T_{eN}} + \lambda \frac{\left||\psi_s^*| - |\vec{\psi}_s(k+1)|_i\right|}{|\vec{\psi}_{sN}|}, \quad i\epsilon\{1,2,3,4;5,6,7,8\} \qquad (17)$$

Whereλ is a measuring factor which finds the relative significance of the torque and stator motion, T_e^* and $|\psi_s^*|$are the future references of torque, and transition at skyline k+1, separately. T_{eN} and $\left|\overrightarrow{\psi_{sN}}\right|$ are the greatness of the appraised torque and stator motion. The factor can be set to 1 if the relative significance of torque and motion is the same [7]. Since the voltage vectors of the two subsystems are free to each other, the cost capacity of the entire framework can be given as takes after

$$J_{0,1} = (J_{grid} + \lambda_L J_{load})_{0,1} \qquad (18)$$

Where J0 is the ideal cost work on account of sharedleg condition of 0, while J1 is the ideal cost work on account of the common leg condition of 1. $\lambda_L$is a measuring factor which speaks to the relative significance of the rectifier and the inverter, and subscript 0/1 demonstrates switch condition of the common leg. Regularly, the measuring factor λ_L is set to

$$\lambda_L = 1 \qquad (19)$$

The last ideal changing blend connected to the fiveleg converter can be created by assessing the cost work J0 and J1 .The flowchart of the plan is given in Figure 3. SG,iand SL,ii ε{0,1},ishows exchanging condition of the sharedleg) are the ideal changing states expected to be connected to the rectifier and inverter.

B. Condition for Independent Control

In five-leg AC-DC-AC converter, the principal input voltage and output voltage can be controlled freely, given that the estimation of the dc-link voltage is satisfactory. Be that as it may, as one leg of the inverter imparted to the rectifier, exchanging systems must give sinusoidal voltage to both inverter and rectifier at the shared leg. In a fault tolerant system, the most vital issue is to accomplish a steady and worthy (likely corrupted) execution. On the off chance that the dc-link voltage is not expanded, the restriction of voltage will bring about the corrupted speed customizable range. The most extreme customizable speed is indicated as takes after.

On account of FCS-MPC, just a single real voltage vector is connected in an exchanging period. Finding the momentary voltage from the reference voltage is unimaginable. Thus, the crucial voltages are approximated. On account of the rectifier, the major voltage with receptive power controlled can be approximated by the virtual motion (VF).

$$\psi_v = \int v_g \, dt \qquad (20)$$

When all is said in done, the parasitic wonders and quantization mistake prompt disparity between the recreated voltages and the acknowledged voltages. The basic of this blunder may prompt wrong outcomes. In this manner, low pass channel (LPF) is used to dispense with this blunder. The high pass channel (HPF) is utilized to make up for the phase move and plentifulness constriction of the LPF. The exchange capacity can be given as

$$\psi_v(s) = \frac{1}{s+k_1\omega_g} \frac{s}{s+k_2\omega_g} v_g(s) \qquad (21)$$

Where k1 and k2 are the cutoff frequency of LPF and HPF, individually. Consequently, the essential input voltage can be given a

$$V_g = \omega_g \psi_v \qquad (22)$$

On account of the inverter, the basic output voltage can be given as

$$V_l = \frac{d\psi_s}{dt} + i_l R_s = j\omega\psi_s + i_l R_s \qquad (23)$$

As the frequency of the inputvoltage is settled, at that point adequacy of the essential input voltage is settled. Along these lines, the biggest amplitude of output voltage for inverter can be given as takes after

$$V_{lm} = V_{max} - V_{gm} \qquad (24)$$

Where Vmax = $u_d/\sqrt{3}$ is the biggest sufficiency of dc-link voltage accessible, Vgm and Vlm is the biggest amplitude of dc-connect voltage accessible for rectifier and inverter, separately. Join with (23), the greatest speed movable range for freely control of the five-leg AC-DC-AC converter-encouraged engine drive can be indicated as takes after.

$$\omega_{em} = \frac{V_{lm} - i_l R_s}{|\vec{\psi}_{eN}|} \qquad (25)$$

Where ω_{em} is the speed confinement for free control of the converter.

C. Overcurrent Constraint

During a few transients, the five-leg converter streams can be impressively high, particularly in the shared leg, which would harm the converter. It is alluring to confine these streams in the five-leg converter. In the traditional technique, the overcurrent security is accomplished by limiting the network and load current independently (i.e., the current of each side is compelled to half of the permitted converter current). For this situation, the output current ability is restricted. If there should be an occurrence of the FCS-MPC plot, this inquiry can be stayed away from. This can be executed by including an extra nonlinear term in the cost work. This nonlinear term produces a high esteem when the

streams surpass as far as possible and equivalent to zero when the ebbs and flows inside the cutoff points. Along these lines, the cost work (16)(17) can be revamped as

$$J_{grid} = \frac{|P^* - P(k+1)_i|}{P_N} + \frac{|Q^* - Q(k+1)_i|}{P_N} + \lambda_\infty f(|\vec{i}_g(k+1)| > i_{max}) \quad (26)$$

$$J_{load} = \frac{|T_e{}^* - T_e(k+1)_i|}{T_{eN}} + \lambda \frac{\left||\psi_s{}^*| - |\vec{\psi}_e(k+1)|_i\right|}{|\vec{\psi}_{eN}|} + \lambda_\infty f(|\vec{i}_l(k+1)| > i_{max}) \quad (27)$$

Whereλ_∞ is a high esteem and f (.) is a legitimate capacity, when the condition is valid, the estimation of the capacity is 1, while the condition is false, the estimation of the capacity is 0. The anticipated transient current of the shared leg can be given

$$\vec{i}_{share}(k+1) = \vec{i}_{g3}(k+1) - \vec{i}_{l3}(k+1) \quad (28)$$

In a drive framework, the execution of the inverter offers need to rectifier framework. In this manner, with regards to the shared leg current imperative, it ought to be added to the rectifier cost work

$$J_{grid} = \frac{|P^* - P(k+1)_i|}{P_N} + \frac{|Q^* - Q(k+1)_i|}{P_N} + \lambda_\infty [f(|\vec{i}_g(k+1)| > i_{max}) + f(|\vec{i}_{share}(k+1)| > i_{max})] \quad (29)$$

IV. CONVENTIONAL PWM CONTROL SCHEME

Keeping in mind the end goal to give a total assessment of the proposed control plot, the customary PWM scheme is led for correlation. The acknowledgment of PWM control scheme depends on the voltage-arranged control (VOC) plot for the rectifier and field-situated control (FOC) scheme for the engine with PWM procedure. Among the few PWM approaches examined in the writing for five-leg approach, it appears that the proposed strategy in [4] delivers less present sounds and gives full dc-bus usage. The entire PWM scheme is delineated in Figure 4. For a reasonable examination, the PWM control scheme is actualized with decoupling term in the engine drive and rectifier to enhance the elements. Keeping in mind the end goal to give the most ideal control execution, the PI current controller is tuned legitimately to give the most ideal control execution and the output of the PI controllers is tweaked utilizing PWM to shape the five-leg exchanging states.

V. AN ADAPTIVE NEURO-FUZZY INFERENCE SYSTEM

A adaptive neuro-fuzzy derivation framework or versatile system based fuzzy deduction framework (ANFIS) is a sort of counterfeit neural system that depends on Takagi–Sugeno fuzzy induction framework. The strategy was produced in the mid 1990s. Since it coordinates both neural systems and fuzzy rationale standards, it can possibly catch the advantages of both in a solitary structure. Its induction framework compares to an arrangement of fuzzy IF–THEN decides that have learning capacity to inexact nonlinear capacities. Thus, ANFIS is thought to be an all inclusive estimator. For utilizing the ANFIS as a part of a more productive and ideal way, one can utilize the best parameters acquired by hereditary calculation.

Simulation Results

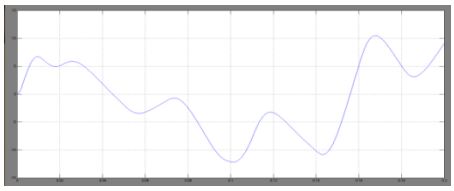

(a)Ishare

Figure 6. Simulation results showing the shared-leg current: (a) with theproposed shared-leg overcurrent constraint.

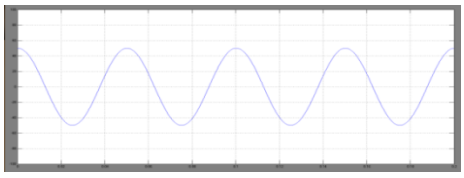

(a)Vl3

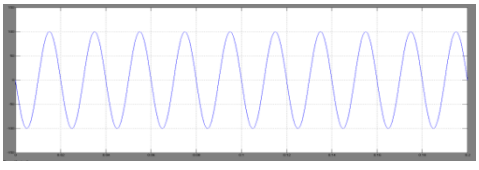

(b)Vg3

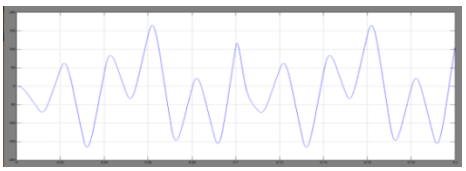

(c)Vg share

Figure 7. Simulation results showing (a) estimated phase l3 output voltage(b) estimated phase g3 input voltage (c) estimated shared-leg voltage.

Using Conventional PWM Scheme:

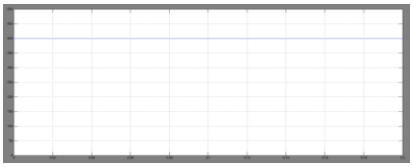

(a)Ud

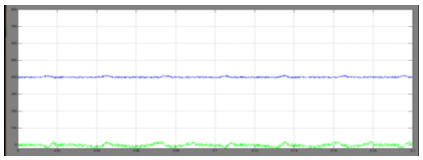

(b)P,Q

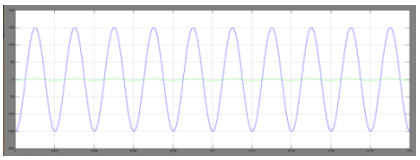

(c)Eg1, ig1

Figure 8. Simulation results showing the steady performance of the fivelegAC-DC-AC scheme: (a)-(c) with the conventional PWM scheme. Traces show [(a)] dc-link voltage, [(b)]active and reactive power, [(c)] phase g1 voltage and current.

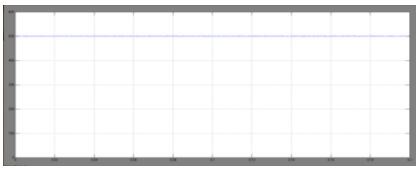

(a)W

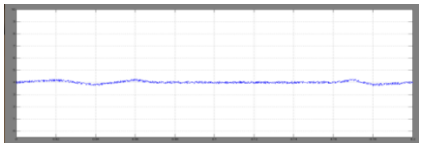

(b)Te

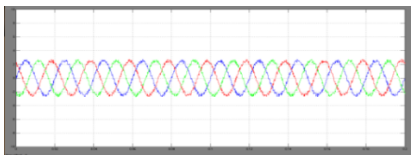

(c)Ilabc

Figure 9. Simulation results showing the steady performance of the fivelegAC-DC-AC scheme: (a)-(c) with the conventional PWM scheme. Traces show [(a)] speed, [(b)] torque, [(c)] three-phase load current.

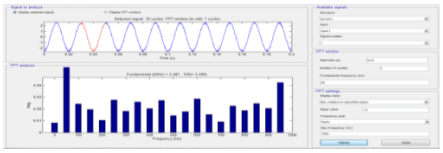

Ig1conv

Figure 10. Simulation results showing the steady performance of the fiveleg
AC-DC-AC scheme: (a),(b) with the conventional PWM scheme. Traces show [(a)] grid phase g1 current, [(b)] spectrum of the grid phase g1 current

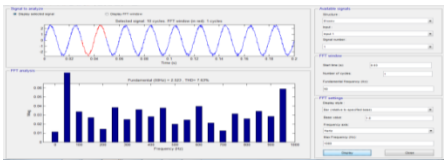

Il1conv

Figure 11. Simulation results showing the steady performance of the fiveleg
AC-DC-AC scheme: (a),(b) with the conventional PWM scheme. Traces show [(a)] motor phase l1 current,[(b)] spectrum of the motor phase l1 current

Case 2a

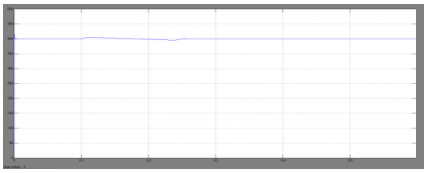

(a)Ud

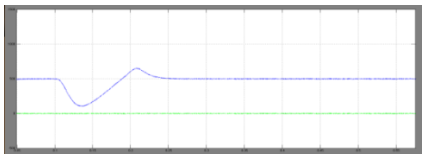

(b)P,Q

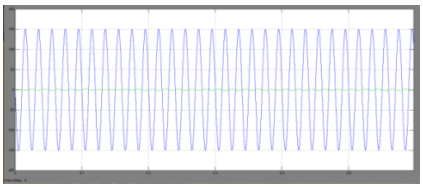

(c)Eg1, ig1

Figure 12. Simulation results showing the dynamic performance of the fiveleg AC-DC-AC scheme during speed reversal maneuver: (a)-(c)with the conventional PWM scheme. Traces show [(a)] dc-link voltage, [(b)] active and reactive power, [(c)] phase g1 voltage and current.

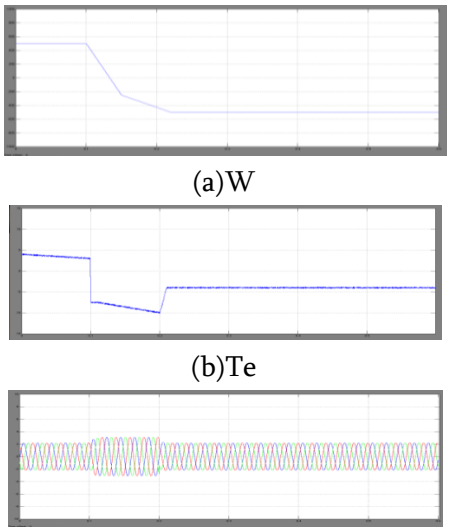

(a)W

(b)Te

(c)Iabc

Figure 13. Simulation results showing the dynamic performance of the fiveleg AC-DC-AC scheme during speed reversal maneuver: (a)-(c) with the conventional PWM scheme. Traces show [(a)] speed, [(b)] torque, [(c)] three-phase current.

Case 2b

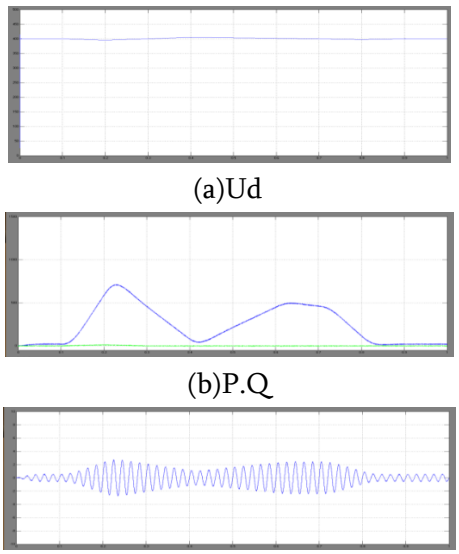

(a)Ud

(b)P.Q

(c)Ig1

Figure 14. Simulation results showing the dynamic performance of the fiveleg AC-DC-AC scheme during load change: (a)-(c) with the conventional PWM scheme. Traces show [(a)] dc-linkvoltage, [(b)] active and reactive power, [(c)] phase g1 current.

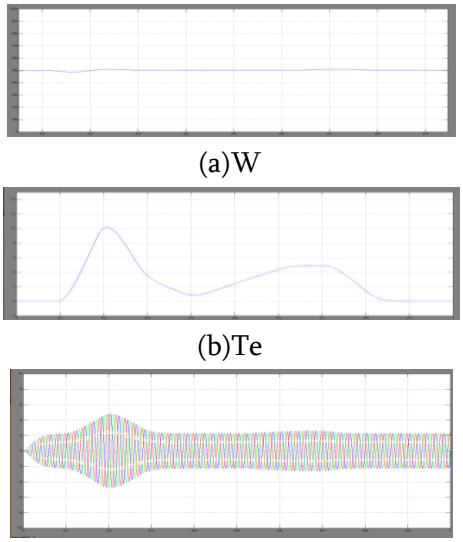

(a)W

(b)Te

(c)Ilabc

Figure 15. Simulation results showing the dynamic performance of the fiveleg AC-DC-AC scheme during load change: (a)-(c) with the conventional PWM scheme. Traces show [(a)] speed, [(b)] torque, [(c)] three-phase current.

Using MPC controller Scheme:

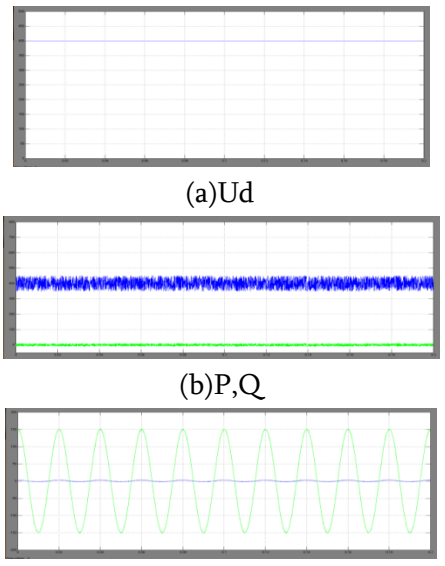

(a)Ud

(b)P,Q

(c)Eg1,ig1

Figure 16. Simulation results showing the steady performance of the fiveleg
AC-DC-AC scheme: (a)-(c) with the proposed MPC scheme. Traces show [(a)] dc-link voltage, [(b)]active and reactive power, [(c)] phase g1 voltage and current.

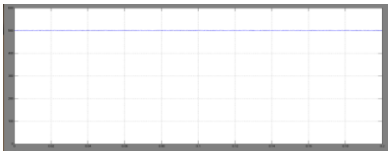

(a)W

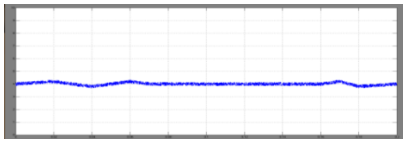

(b)Te

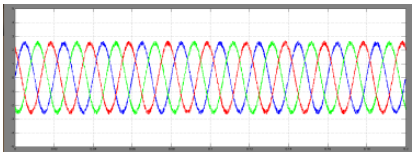

(c)Ilabc

Figure 17. Simulation results showing the steady performance of the fiveleg

AC-DC-AC scheme: (a)-(c) with the proposed MPC. Traces show [(a)] speed, [(b)] torque, [(c)] three-phase load current.

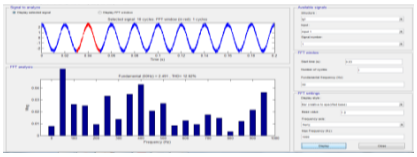

Ig1 proposed

Figure 18. Simulation results showing the steady performance of the fiveleg

AC-DC-AC scheme: (a),(b) with the MPC scheme. Traces show [(a)] grid phase g1 current, [(b)] spectrum of the grid phase g1 current

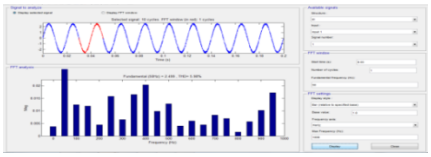

Il1 proposed

Figure 19. Simulation results showing the steady performance of the fiveleg

AC-DC-AC scheme: (a),(b) with the MPC scheme. Traces show [(a)] motor phase l1 current,[(b)] spectrum of the motor phase l1 current

Case2a

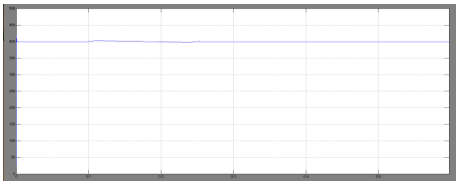

(a)Ud

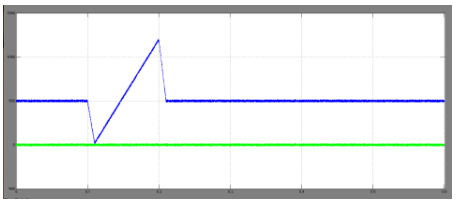

(b)P,Q

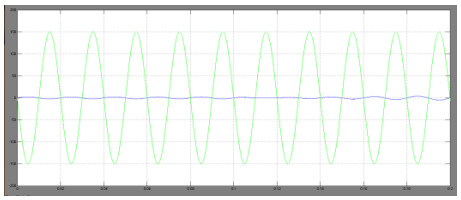

(c)Eg1,ig1

Figure 20. Simulation results showing the dynamic performance of the fiveleg AC-DC-AC scheme during speed reversal maneuver: (a)-(c)with the MPC scheme. Traces show [(a)] dc-link voltage, [(b)] active and reactive power, [(c)] phase g1 voltage and current.

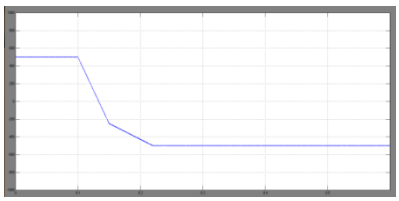

(a)W

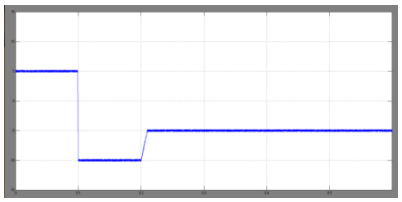

(b)Te

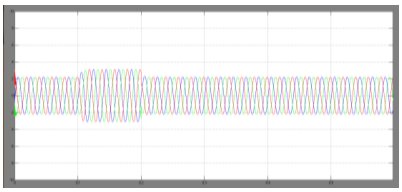

(c)Ilabc

Figure 21. Simulation results showing the dynamic performance of the fiveleg AC-DC-AC scheme during speed reversal maneuver: (a)-(c) with the MPC scheme. Traces show [(a)] speed, [(b)] torque, [(c)] three-phase current.

Case 2b

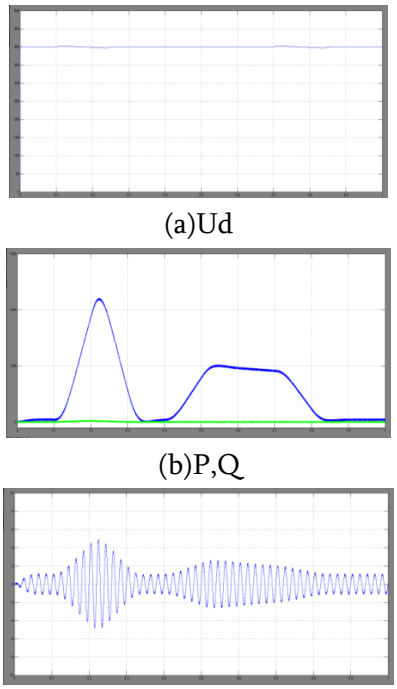

(a)Ud

(b)P,Q

(c)Ig1

Figure 22. Simulation results showing the dynamic performance of the fiveleg AC-DC-AC scheme during load change: (a)-(c) with the MPC scheme. Traces show [(a)] dc-linkvoltage, [(b)] active and reactive power, [(c)] phase g1 current.

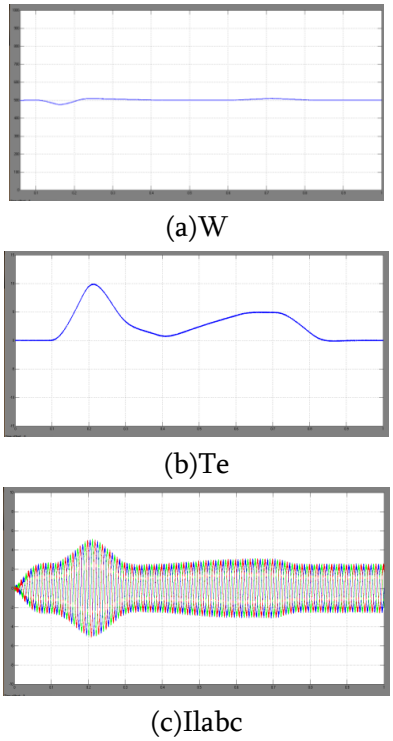

(a)W

(b)Te

(c)Ilabc

Figure 23. Simulation results showing the dynamic performance of the fiveleg AC-DC-AC scheme during load change: (a)-(c) with the MPC scheme. Traces show [(a)] speed, [(b)] torque, [(c)] three-phase current.

Using ANFIS controller Scheme:

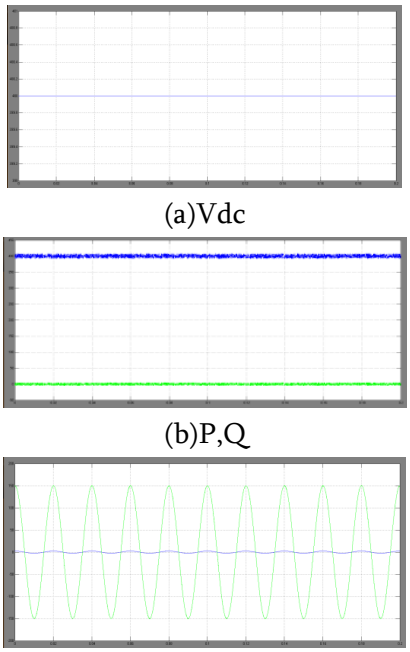

(a)Vdc

(b)P,Q

(c)Eg1,ig1

Figure 24. Simulation results showing the steady performance of the fivelegAC-DC-AC scheme: (a)-(c) with the proposed MPC scheme. Traces show [(a)] dc-link voltage, [(b)]active and reactive power, [(c)] phase g1 voltage and current.

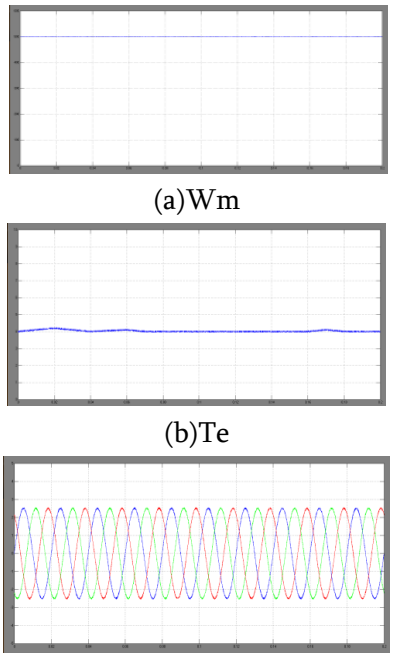

(a)Wm

(b)Te

(c)Ilabc

Figure 25. Simulation results showing the steady performance of the fivelegAC-DC-AC scheme: (a)-(c) with the ANFIS scheme. Traces show [(a)] speed, [(b)] torque, [(c)] three-phase load current.

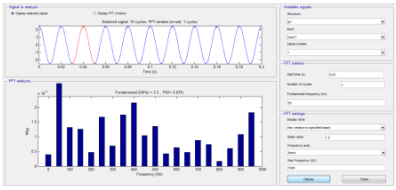

Figure 26. Simulation results showing the steady performance of the fiveleg
AC-DC-AC scheme: (a),(b) with the ANFIS scheme. Traces show [(a)] grid phase g1 current, [(b)] spectrum of the grid phase g1 current

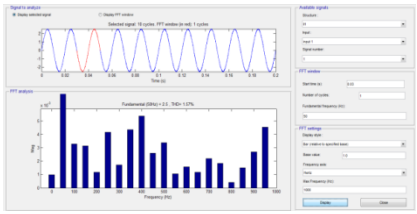

Figure 27. Simulation results showing the steady performance of the fivelegAC-DC-AC scheme: (a),(b) with the ANFIS scheme. Traces show [(a)] motor phase l1 current,[(b)] spectrum of the motor phase l1 current

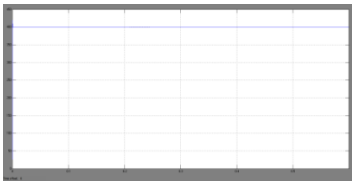

(a)Udc

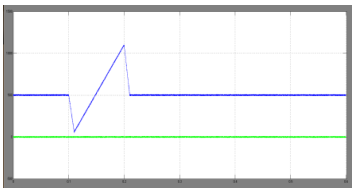

(b)P,Q

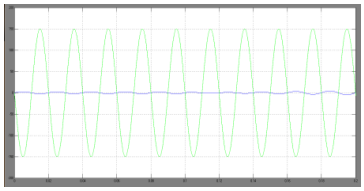

(c)Ig1,eg1

Figure 28. Simulation results showing the dynamic performance of the fiveleg AC-DC-AC scheme during speed reversal maneuver: (a)-(c)with the ANFIS scheme. Traces show [(a)] dc-link voltage, [(b)] active and reactive power, [(c)] phase g1 voltage and current.

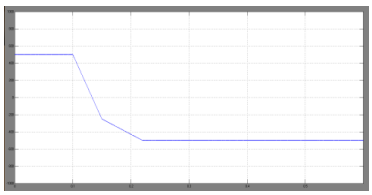

(a)Wm

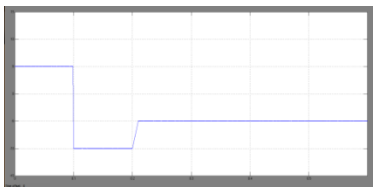

(b)Te

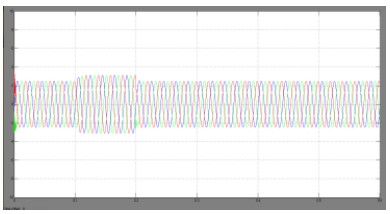

(c)Ilabc

Figure 29. Simulation results showing the dynamic performance of the fiveleg AC-DC-AC scheme during speed reversal maneuver: (a)-(c) with the ANFIS scheme. Traces show [(a)] speed, [(b)] torque, [(c)] three-phase current.

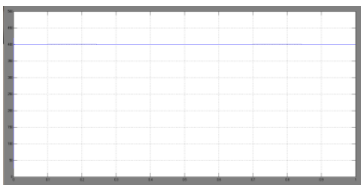

(a)Vdc

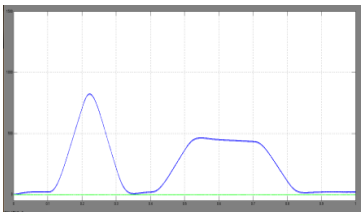

(b)P,Q

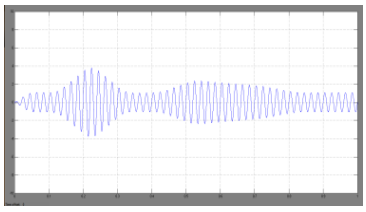

(c)Ig1

Figure 30. Simulation results showing the dynamic performance of the fiveleg AC-DC-AC scheme during load change: (a)-(c) with the ANFIS scheme. Traces show [(a)] dc-linkvoltage, [(b)] active and reactive power, [(c)] phase g1 current.

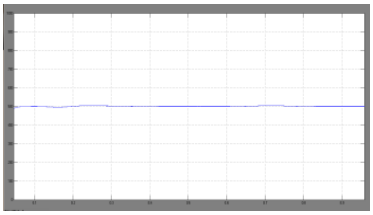

(a)Wm

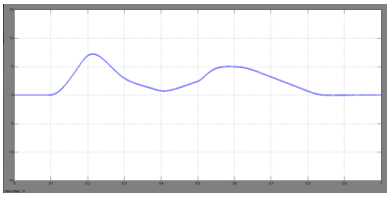

(b)Te

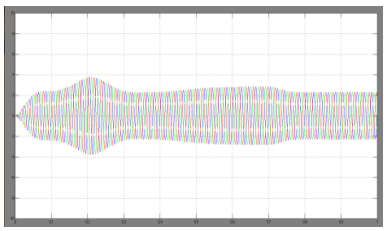

(c)Ilabc

Figure 31. Simulation results showing the dynamic performance of the fiveleg AC-DC-AC scheme during load change: (a)-(c) with the ANFIS scheme. Traces show [(a)] speed, [(b)] torque, [(c)] three-phase current.

VI. CONCLUSION

In this paper, the usage of a five-leg AC-DC-AC converter-fed induction motor has been explained. A new control scheme in light of the ANFIS is joined with inherent normal for the five-leg converter is proposed for free control of the rectifier and inverter subsystem with the shared leg overcurrent limitation. The autonomous control condition for the five-leg AC-DC-AC converter is broke down. In the proposed sheme, the required number of controllers is lessened from the traditional four to one prescient controller and factor tuning exertion is spared. In spite of the fact that it has been confirmed in the analysis that the traditional PWM control plan can give even a superior execution with bring down THD of the rectifier current, it is trusted that the accomplished execution of the proposed FCS-MPC is as yet tasteful while giving quicker transient execution and a decent approach to manage the common leg overcurrent. With the proposed ANFIS, the five-leg converter-sustained induction motor has been observed to be competent to enhance the reliability quality of the AC-DC-AC drive framework and gives dynamic performances and good results than existing scheme of FCS-MPC.

VII. REFERENCES

[1]. M. Malinowski, M. Kazmierkowski, and A. Trzynadlowski, "A comparativestudy of control techniques for PWM rectifiers in AC adjustablespeed drives," IEEE Trans. Power Electron., vol. 18, no. 6, pp. 1390–1396, 2003.

[2]. B. Mirafzal, "Survey of fault-tolerance techniques for three-phase voltagesource inverters," IEEE Trans. Ind. Electron., vol. 61, no. 10, pp.5192–5202, 2014.

[3]. C. Cecati, A. Di Tommaso, F. Genduso, R. Miceli, and G. RiccoGalluzzo,"Comprehensive modeling and experimental testing of faultdetection and management of a nonredundant fault-tolerant vsi," IEEETrans. Ind. Electron., vol. 62, no. 6, pp. 3945–3954, 2015.

[4]. M. Jones, S. Vukosavic, D. Dujic, E. Levi, and P. Wright, "Five-leginverter PWM technique for reduced switch count two-motor constantpower applications," IET Elect. Power Appl., vol. 2, no. 5, pp. 275–287,2008.

[5]. A. Bouscayrol, B. Francois, P. Delarue, and J. Niiranen, "Control implementation of a five-leg AC-ac converter to supply a three-phase induction machine," IEEE Trans. Power Electron., vol. 20, no. 1, pp. 107–115, 2005.

[6]. Y. Zhang and H. Yang, "Model-predictive flux control of induction motor drives with switching instant optimization," IEEE Trans. Energ.Convers., vol. 30, no. 3, pp. 1113–1122, 2015.